Journal of Cellular Biochemistry 80:248–258 (2000)

Differential Insulin-Like Growth Factor (IGF)-Independent Interactions of IGF Binding Protein-3 and IGF Binding Protein-5 on Apoptosis in Human Breast Cancer Cells. Involvement of the Mitochondria.

C. M. Perks,* C. McCaig, and J. M. P. Holly

Division of Surgery, Department of Hospital Medicine, Bristol Royal Infirmary, Bristol, BS2 8HW, United Kingdom

Abstract We have demonstrated previously in Hs578T cells that insulin-like growth factor binding protein (IGFBP)-3 can significantly accentuate ceramide (C2)-induced apoptosis, but has no effect on cell death induced by integrin detachment [using an arginine-glycine-aspartic acid (RGD)-containing peptide]. In contrast we found that IGFBP-5 could inhibit apoptosis induced by either C2 or integrin detachment. It is now clear that the mitochondria not only provide the energy required for cell viability, but can also play an important role during the commitment phase to apoptosis. We used a mitochondrial respiratory chain inhibitor, antimycin A, at both apoptotic and nonapoptotic doses to further investigate the IGF-independent actions of IGFBP-3 and IGFBP-5 on C2 and RGD-induced apoptosis in the Hs578T cells. Hs578T cells had one of three treatments. 1: They were incubated with increasing doses of antimycin A for 24 h. 2: They were coincubated with an apoptotic dose of either C2 or RGD together with a nonapoptotic dose of antimycin A for 24 h. 3: They were incubated with a binding protein (100 ng/ml) for 24 h followed by coincubation of the binding protein with an apoptotic dose of antimycin A for a further 24 h. Cell viability was assessed by trypan blue dye exclusion and MTT assay, and apoptosis was confirmed and measured by morphologic assessment and flow cytometry. We found that antimycin A initiated apoptosis at 10 μmol/L and above. We also demonstrated that a nonapoptotic dose of antimycin A (0.1 μmol/L) significantly inhibited C2-induced apoptosis, whereas it significantly accentuated RGD-induced cell death. In addition, we found that cell death induced by antimycin A can be accentuated by IGFBP-3 but is not affected by IGFBP-5. These data indicate that IGFBP-3 can directly enhance apoptosis triggered via the mitochondria; either directly by a mitochondrial inhibitor or by C2 (which we demonstrate to act via effects on the mitochondria in this model). IGFBP-5, however, appears to confer survival effects via a distinct pathway not involving the mitochondria. J. Cell. Biochem. 80:248–258, 2000.

Key words: apoptosis; mitochondria; insulin-like growth factor–binding proteins

Tissue homeostasis in a multicellular organism is maintained via a balance between cell proliferation and programmed cell death. Apoptosis is a highly regulated mode of cell death that is characterised by a number of morphologic and biochemical features including blebbing of the plasma membrane, cell shrinkage, chromatin condensation, and DNA fragmentation into membrane-bound vesicles [Wyllie et al., 1980].

We have been using two physiologic inducers of apoptosis, namely a ceramide analogue (C2) and a synthetic arginine-glycine-aspartic acid-containing peptide (RGD), to investigate the modulation of cell survival by insulin-like growth factor (IGF) system components. Sphingomyelin hydrolysis occurs in the plasma membrane, and is now recognised as an important pathway of signal transduction. Ceramide is one product of sphingomyelin hydrolysis and has been implicated as an important mediator of cell death [Obeid et al., 1993]. Tumour growth can be restricted by cytokines, chemotherapy, and radiotherapy, which induce programmed cell death via ceramide-mediated cytoplasmic signalling.

Grant sponsors: Medical Research Council and Wellcome Trust.

*Correspondence to: C. M. Perks, Division of Surgery, Department of Hospital Medicine, Bristol Royal Infirmary, Bristol, BS2 8HW, England, UK.

Received 3 March 2000; Accepted 4 July 2000

The growth of normal adherent cell types in vitro requires soluble signals (such as growth factors) and attachment to the extracellular matrix (ECM) [Ingber, 1990]. Cell adhesion to the ECM is mediated by integrin receptors. These bind to matrix proteins outside the cell and associate with cytoskeletal proteins within the cell. Many of these matrix proteins contain the three amino acid sequence arginine-glycine-aspartic acid (RGD), which is specifically recognised by its particular integrin receptor [Ruoslahti and Pierschbacher, 1987]. Integrin-dependent signals have been shown to modulate the control of growth [Giancotti and Ruoslahti, 1990] and cell survival [Frisch and Francis, 1994]. It has been demonstrated previously that disruption of these attachments, via addition of antibodies or peptides, can induce cells to detach from the substratum [Knudson et al., 1981; Hayman et al., 1985] with a resultant induction of programmed cell death. Cells that become transformed or malignant have acquired the ability to undergo anchorage-independent growth [Freedman et al., 1974; Tucker et al., 1981].

For many cell types the most potent external soluble signals opposing apoptosis are the IGFs. The IGFs are generally present in excess but their availability to cell receptors is limited by the presence of soluble high-affinity binding proteins (IGFBPs). It has recently become clear, however, that these IGFBPs may also have direct intrinsic actions on cell growth and survival.

The Hs578T cells provide an ideal model in which to study the IGF-independent effects of the IGFBPs because they are nonresponsive to IGFs in terms of cell survival or mitogenesis [Oh et al., 1993]. We have demonstrated previously that C2 and RGD induce dose-dependent apoptosis in these cells. In addition, IGFBP-3 can accentuate C2-induced cell death, but not that initiated by RGD; whereas IGFBP-5 (despite its structural similarity to IGFBP-3) can significantly inhibit apoptosis induced by both triggers [Gill et al., 1997; Perks et al., 1999a]. Furthermore, we have also shown that IGFBP-3 can also accentuate both UV- and paclitaxel- induced apoptosis in these and other epithelial cells in an IGF-independent manner [Fowler et al., 1999; Hollowood et al., 1999].

Within the cell, the mitochondria supply the energy required for cell viability. However, it is becoming increasingly evident that mitochondria also play an important role in the commitment phase of apoptosis [Green and Amarante-Mendes, 1998]. Indeed it has recently been proposed that there are two different pathways leading to apoptosis, a direct path utilising caspase-8 and -3 and an alternative indirect pathway involving the mitochondria [Scaffidi et al., 1999]. Because the mitochondria play such a key role in the regulation of apoptosis [Green and Amarante-Mendes, 1998], we have employed a mitochondrial respiratory chain inhibitor (antimycin A) that has a specific inhibitor-binding site near the high potential haem group of cytochrome b. The cytochrome bc1 is one of the three major respiratory enzyme complexes residing in the inner mitochondrial membrane. Cytochrome bc1 transfers electrons from ubiquinol to cytochrome c and uses the energy released to form an electrochemical gradient across the inner membrane [Zhang et al., 1998].

The goals of this study initially were to use antimycin A at nonapoptotic doses to investigate its effects on C2 and RGD-induced programmed cell death. Secondly, we also investigated the role of the mitochondria in IGFBP-3 and -5 actions in these cells because recent evidence indicated two distinct signalling pathways for apoptosis, either directly or indirectly via the mitochondria [Scaffidi et al., 1999] and we have previously shown that IGFBP-3 and IGFBP-5 had differential effects on apoptosis induced by different triggers [Perks et al., 1999a].

MATERIALS AND METHODS

Recombinant human nonglycosylated IGFBP-3 was a kind gift from Dr. C. Maack, Celtrix, CA. IGFBP-5 was purchased from Austral Biologicals. The ceramide analogue C2 was from Calbiochem and the synthetic RGD-containing peptide (Gly-Arg-Gly-Asp-Thr-Pro) was from Sigma. For negative controls we used the ceramide analogue D-*erythro*-Sphingosine, Dihydro-, N-Acetyl- and a synthetic RGE-containing peptide (Arg-Gly-Glu-Ser) that we had previously shown to have no effect in this cell line (Perks et al., 1999b). Mitotracker was purchased from Molecular Probes, Eugene, OR. All other chemicals were purchased from Sigma. Tissue culture plastics were obtained from Nunc, Gibco Life Technologies, Paisley, Scotland.

Cell Culture

The human breast cancer cell line Hs578T was purchased from ECACC, Porton Down, Wiltshire and was grown in a humidified 5% CO_2 atmosphere at 37°C. Cells were maintained in growth media (GM) containing Dulbecco's modified Eagle's medium (DMEM) with glutamax-1 supplemented with 10% foetal calf-serum, penicillin (5,000 IU/ml), and streptomycin (5 mg/ml). Experiments were performed on cells in phenol-red-free, serum-free DMEM and Ham's nutrient mix F-12 (SFM) with sodium bicarbonate (0.12%), bovine serum albumin (0.2 mg/ml), transferrin (0.01 mg/ml), and supplemented as before.

Dosing Protocol

Cells were grown in GM for 24 h before switching to SFM for a further 24 h prior to dosing, when cells were approximately 80%–90% confluent. Cells had one of three treatments.

1. They were incubated with increasing doses of antimycin A for 24 h.
2. They were coincubated with an apoptotic dose of either C2 or RGD together with a nonapoptotic dose of antimycin A for 24 h.
3. They were preincubated with a binding protein (100 ng/ml) for 24 h followed by coincubation of the binding protein with an apoptotic dose of antimycin A for an additional 24 h.

We have established previously that 100 ng/ml of binding protein was the optimum dose for interaction with C2 or RGD-induced apoptotic signalling pathways [Gill et al., 1997; Perks et al., 1999a].

Mitotracker Staining

Following trypsinisation, both adherent and nonadherent cells were collected for analysis. Cells were resuspended in mitotracker dye (150 nM; 500 μl) and incubated at 37°C for 20 min according to manufacturer's instructions. The cells were spun down and the supernatant was discarded. The cells were washed in phosphate-buffered saline (PBS) and fixed in 10% formal saline for 10 min at room temperature. The cells were spun down, PBS-washed, and stored at 4°C prior to analysis of mitochondrial activity using the flow cytometer.

MTT Assay

MTT reagent (3-[4,5-dimethylthiazol-2-yl]-2,5-diphenyltetrazolium bromide) is converted into a coloured water-insoluble formazan salt by the metabolic activity of viable cells and can be used as a crude measure of cell viability. Cells were seeded at 2.5×10^4/ml (150 μl GM) in 96-well plates and were allowed to grow for 24 h. Growth medium was replaced with SFM (100 μl) 24 h prior to dosing. MTT reagent (7.5 mg/ml; PBS) was added to the cells (10 μl/well) and the cultures were incubated for 30 min at 37°C. The reaction was stopped by the addition of acidified triton buffer [0.1 M HCl, 10% (v/v) Triton X-100; 50 μl/well] and the tetrazolium crystals were dissolved by mixing on a Titertek plate shaker for 20 min at room temperature. The samples were measured on a Biorad 450 plate reader at a test wavelength of 595 nm and a reference wavelength of 650 nm.

Trypan Blue Dye Exclusion

Aliquots of cells (50 μl) were loaded onto a haemocytometer (1:1) with trypan blue (50 μl). Total cell number was counted and dead cells were specifically identified as those that had taken up the blue dye. The percentage of dead cells was then calculated.

Flow Cytometry

This technique was used to confirm and measure the amount of apoptosis in a given sample of cells. Both adherent and nonadherent cells were collected for analysis. In apoptotic cells, fragmented DNA was washed out of fixed cells resulting in lower DNA staining of the cells that appear as a pre-G1 peak following cell cycle analysis. Cells ($1–2 \times 10^6$) were washed in PBS and fixed for 30 min by the addition of 70% ethanol (1 ml). Cells were pelleted (2,000 rpm for 5 min) and washed three times with PBS. The supernatant was removed and the cells were resuspended in reaction buffer (propidium iodide, 0.05 mg/ml; sodium citrate, 0.1%; RNAse A, 0.02 mg/ml; NP-40, 0.3%; pH 8.3), vortexed, and incubated at 4°C for 30 min. All cells were then measured on a FACSCALIBUR flow cytometer (Becton Dickinson) with an argon laser at 488 nm for excitation and analysed using Cell Quest (Becton Dickinson).

Morphologic Assessment

To establish that antimycin A-induced cell death gave rise to the classic morphologic features associated with apoptosis, aliquots of treated and untreated cells were cytospun and stained with Wright's stain in an automated stainer [Lillie et al., 1977]. Photomicrographs of cells were taken under oil immersion at a magnification of ×100. To assess changes in the levels of attached versus floating cells, they were viewed under phase contrast with ×20 objective optics and images were captured using a JVC TK 1281 colour video camera coupled to time lapse video-recording software Adobe Premiere 4.1.

Statistical Analysis

The data were analysed using the Microsoft Excel 5 software package. Significance was determined using analysis of variance. A statistically significant difference was considered to be present at $P < 0.05$.

RESULTS

Nonapoptotic and Apoptotic Doses of Antimycin A

We first established the changes in metabolic activity of Hs578T human breast cancer cell lines in response to addition of increasing doses of antimycin A. The MTT assay was used initially as a crude measure of cell viability. Figure 1A shows that the metabolic activity in response to antimycin A (0–50 μmol/L) induced a dose-dependent decrease in metabolic activity of the Hs578T human breast cancer cell line. Cell counting using trypan blue dye exclusion (Fig. 1A) indicated that no significant cell death was occurring at antimycin A doses up to and including 2 μmol/L. However, significant ($P < 0.001$) cell death was initiated at doses of 5 μmol/L and above.

Using the mitotracker dye, we determined that 0.1 μmol/L antimycin A, although not affecting cell viability, still elicited a 45% inhibition of mitochondrial activity relative to untreated cells. Maximal inhibition of mitochondrial activity was seen with doses of 0.5 μmol/L and higher (Fig. 1B).

We subsequently used antimycin A at 0.1 μmol/L as a nonapoptotic dose and at 10 μmol/L as an apoptotic dose for all further experiments. We confirmed the ability of antimycin A (10 μmol/L) to induce apoptosis via morphologic analysis that indicated some of the classic features associated with apoptosis (Fig. 1C). Cell shrinkage, cytoplasmic condensation, and formation of apoptotic bodies were evident.

Antimycin A Inhibits C2-Induced Apoptosis

Trypan blue dye exclusion was used to measure the percentage of dead Hs578T cells following treatment with an apoptotic dose of C2 alone, a nonapoptotic dose of antimycin A (0.1 μmol/L) alone, and the combination of both treatments (Fig. 2A). Data showed that antimycin A alone had no effect on cell death relative to control cells. Ceramide, however, induced marked cell death and this was significantly ($P < 0.05$) inhibited on coincubation with antimycin A.

The same profile was seen using flow cytometry where apoptotic cells are seen as a pre-G1 peak (Fig. 2B). Antimycin A alone had no effect on apoptosis relative to control cells, C2 caused a dramatic increase in programmed cell death, which was again significantly ($P < 0.05$) inhibited by antimycin A.

Antimycin A Accentuates RGD-Induced Apoptosis

We used trypan blue dye exclusion to measure the percentage of dead Hs578T cells compared to control untreated cells following treatment with an apoptotic dose of RGD alone, a nonapoptotic dose of antimycin A (0.1 μmol/L) alone, and the combination of both treatments. Data showed that antimycin A alone had no effect on cell death relative to control cells. RGD alone induced a marked increase in cell death and this was significantly ($P < 0.01$) accentuated on coincubation with antimycin A (Fig. 3A). Similarly, Fig. 3B shows the same profile where antimycin A alone had no effect on apoptosis relative to control cells, RGD caused an increase in apoptotic cells that was again significantly ($P < 0.01$) accentuated by antimycin A.

Morphological Assessment of Antimycin A on C2- and RGD-Induced Apoptosis

Morphologic evidence (Fig. 4) provides further support for the antimycin A attenuation of C2-induced apoptosis and accentuation of RGD-induced programmed cell death in the Hs578T

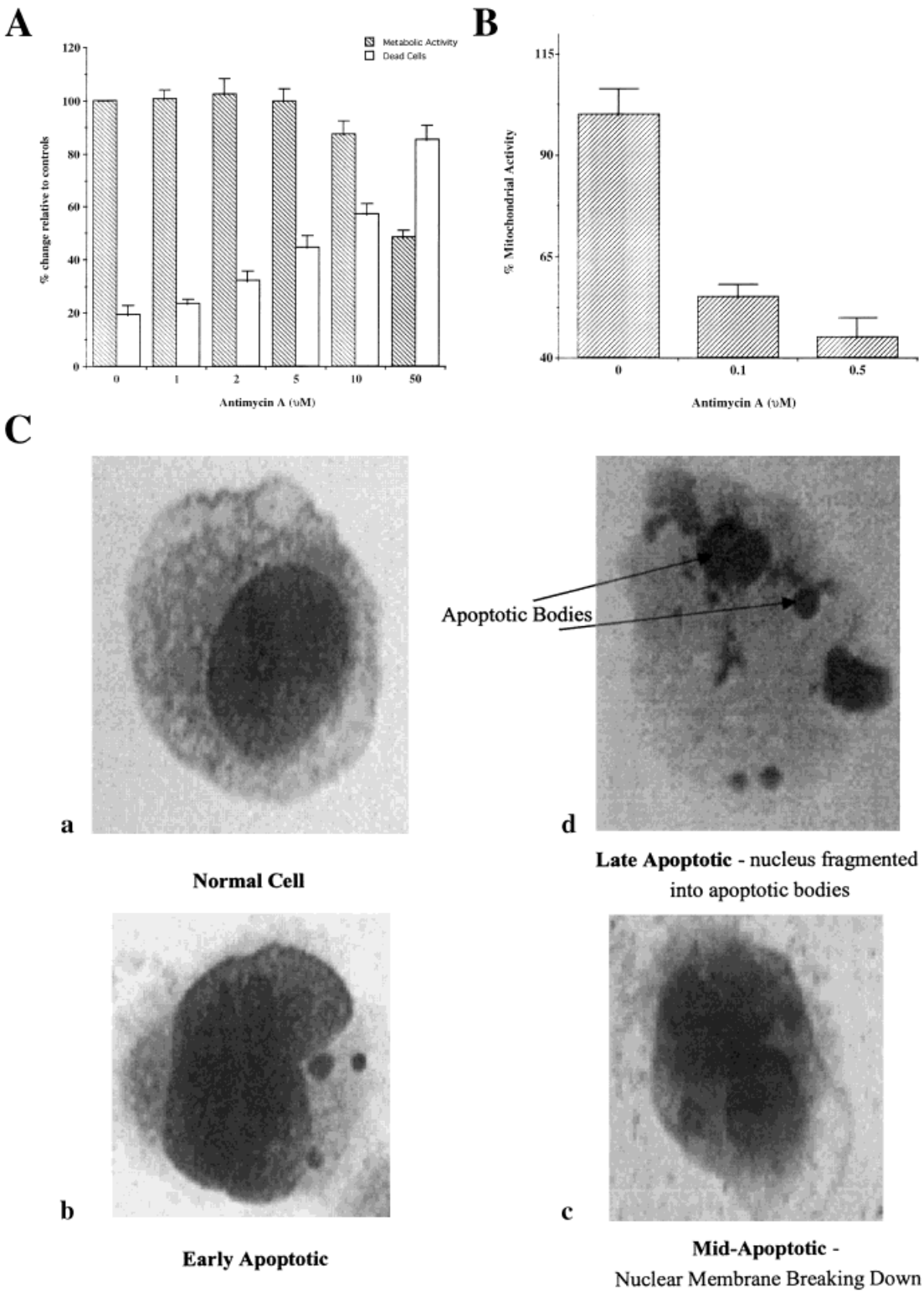

Fig. 1. Characterisation of nonapoptotic and apoptotic doses of antimycin A in the Hs578T human breast cancer cells. **A:** Effects of antimycin A (0–50 μmol/L) on the metabolic activity and percentage of dead Hs578T cells after treatment for 24 h. Cells were seeded in 96-well plates and six-well plates and all were switched to serum-free Dulbecco's modified Eagle's medium and Ham's nutrient mix F-12 (SFM) prior to treatment. MTT activity was assayed as described in Materials and Methods and the results represent the mean ± SEM of five wells from one experiment that is representative of experiments repeated at least three times. Trypan blue dye exclusion was used to measure percentage of dead cells, and graphs show the mean of data from at least three experiments that were each performed in triplicate. **B:** This graph represents the percentage change in metabolic activity as measured using a specific mitochondrial dye (mitotracker) of Hs578T cells after treatment with antimycin A (0–50 μmol/L). **C:** Photomicrographs of control cells (**a**) and those treated with an apoptotic dose of antimycin A (10 μmol/L). (**b**) An early apoptotic cell. (**c and d**) Mid-to-late apoptotic cells indicating apoptotic bodies. Cells were cytospun and stained with Wright stain in an automated stainer [Lillie et al., 1977].

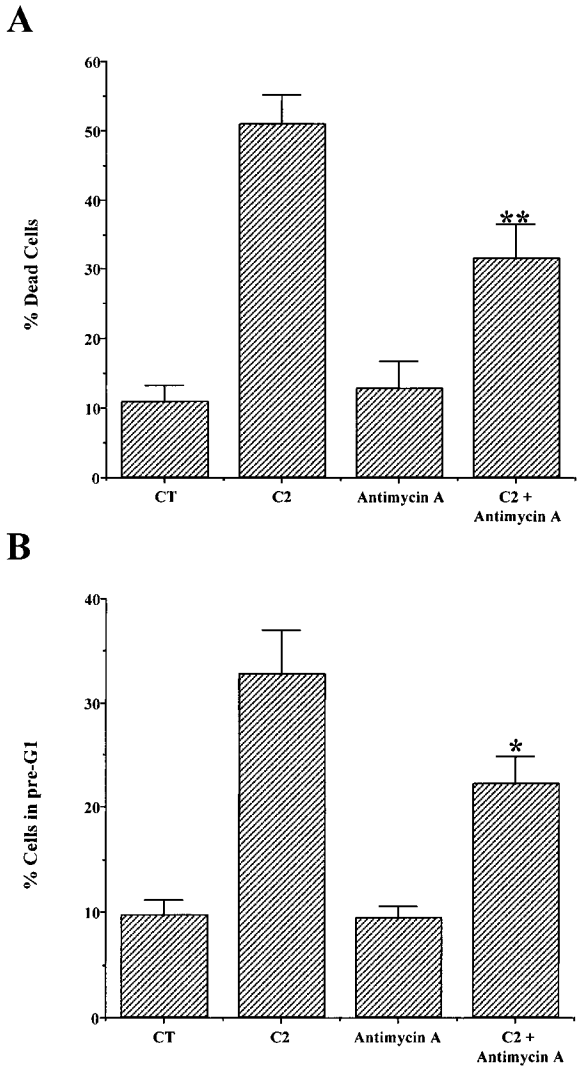

Fig. 2. Effects of Antimycin A at a nonapoptotic dose (0.1 μmol/L) on ceramide-induced apoptosis in the Hs578T human breast cancer cells. Graphs represent the percentage of dead cells (**A**) and cells in the pre-G1 peak (**B**) of untreated cells, C2 alone (7 μmol/L), antimycin A alone (0.1 μmol/L), and C2 plus antimycin A where C2 plus antimycin A is less than C2 alone. Graphs show the mean of data from at least three experiments that were each performed in triplicate. $^{**}P < 0.01$; and $^{*}P < 0.05$.

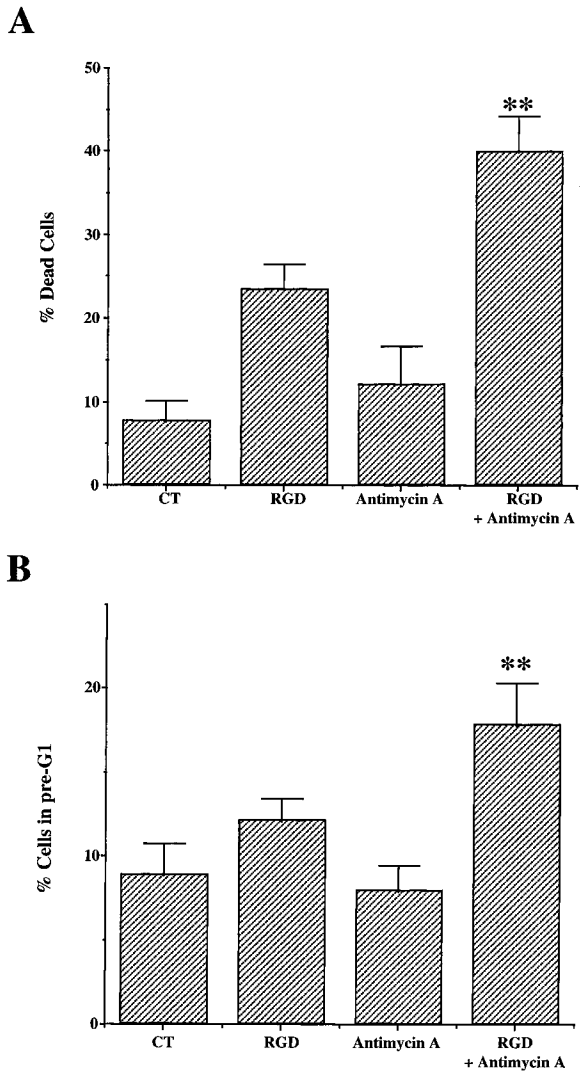

Fig. 3. Antimycin A at a nonapoptotic dose (0.1 μmol/L) accentuated arginine-glycine-aspartic acid (RGD)-induced apoptosis in the Hs578T human breast cancer cells. Graphs represent the percentage of dead cells (**A**) and cells in the pre-G1 peak (**B**) of untreated cells, RGD alone (75 μg/ml), antimycin A alone (0.1 μmol/L), and RGD plus antimycin A where RGD plus antimycin A is greater than RGD alone. Graphs show the mean of data from at least three experiments that were each performed in triplicate ($^{**}P < 0.01$).

cells. Panel I of Figure 4 demonstrates normal, untreated control Hs578T cells. Panel II shows the addition of a nonapoptotic dose of antimycin A (0.1 μmol/L) indicating no effect on the cells relative to controls. Panel III represents cells 24 h following treatment with an apoptotic dose of C2 (7 μmol/L). This illustrates distinct rounding of the cells and a reduction in overall number due to cell detachment. Panel IV shows coincubation of C2 with antimycin A. The number of apoptotic cells in comparison to C2 alone (III) is dramatically reduced with a much higher proportion of live, attached cells still remaining. Panel V represents cells 24 h following treatment with an apoptotic dose of RGD (75 μg/ml). This illustrates a distinct honeycomb effect of the cells and a reduction in overall number due to cell detachment. Panel VI shows coincubation of RGD with antimycin A. The number of apoptotic cells compared to RGD alone (V) is dramatically increased

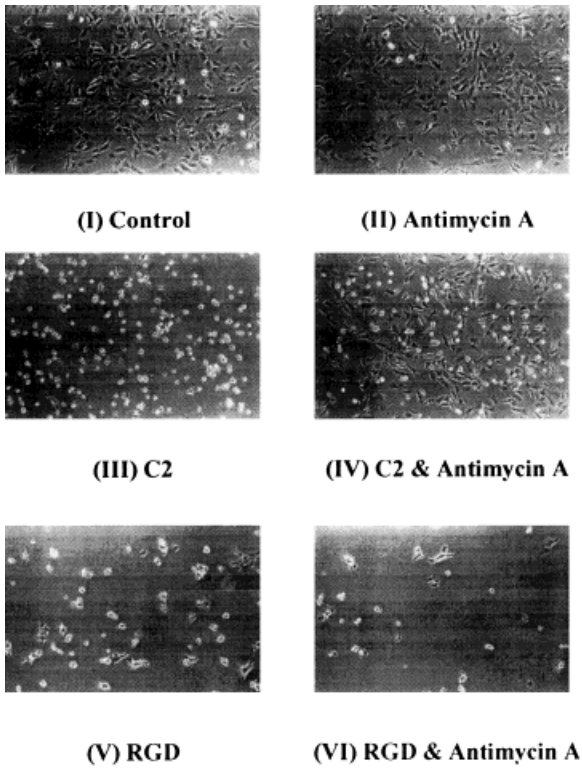

Fig. 4. Morphologic assessment of the effects of a nonapoptotic doses of antimycin A (0.1 μmol/L) on ceramide (C2) and arginine-glycine-aspartic acid (RGD)-induced apoptosis. **Panel I:** Normal, untreated control Hs578T cells. **Panel II:** Cells after the addition of a nonapoptotic dose of antimycin A. **Panel III:** Cells 24 h following treatment with an apoptotic dose of C2 (7 μmol/L). **Panel IV:** Cells coincubated with C2 and antimycin A. **Panel V:** Cells 24 h following treatment with an apoptotic dose of RGD (75 μg/ml). **Panel VI:** Cells coincubated with RGD and antimycin A.

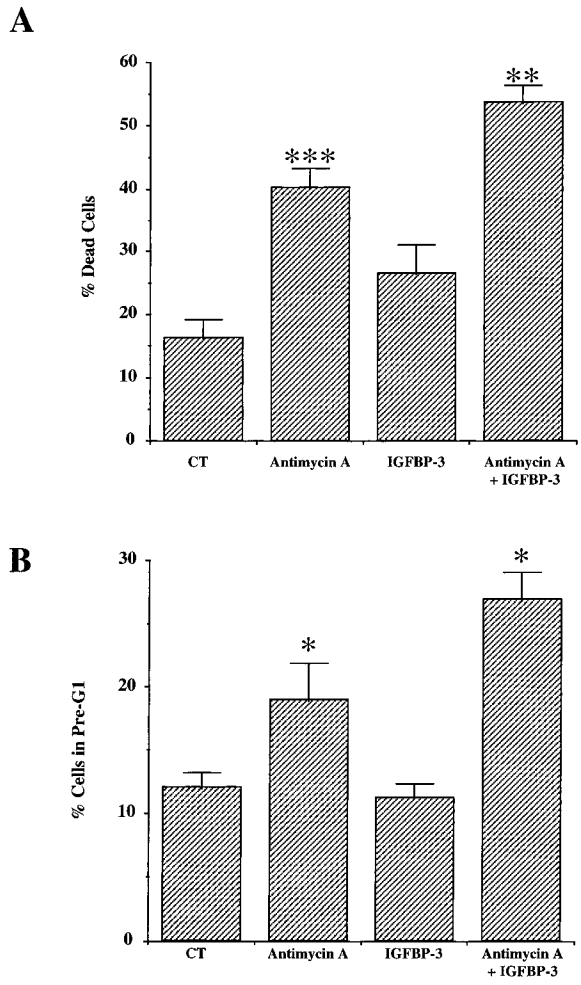

Fig. 5. Insulin-like growth factor binding protein-3 (IGFBP-3) accentuates an apoptotic dose of antimycin A in the Hs578T human breast cancer cells. Graphs represent the percentage of dead cells (**A**) and cells in the pre-G1 peak (**B**) of untreated cells, antimycin A alone (10 μmol/L), IGFBP-3 alone (100 ng/ml), and antimycin A and IGFBP-3 where antimycin A is greater than controls and antimycin A plus IGFBP-3 is greater than antimycin A alone. Graphs show the mean of data from at least three experiments that were each performed in triplicate. $^{*}P < 0.05$; $^{**}P < 0.01$, and $^{***}P < 0.001$.

with a much lower proportion of live, attached cells still remaining.

IGFBP-3 Accentuates an Apoptotic Dose of Antimycin A

We used trypan blue dye exclusion to measure the percentage of dead cells compared to untreated control cells following treatment with an apoptotic dose of antimycin A alone, IGFBP-3 (100 ng/ml) alone, and the combination of both treatments. Data showed that antimycin A alone caused a significant ($P < 0.001$) increase in dead cells, whereas IGFBP-3 alone had no effect relative to controls. However, when used together IGFBP-3 caused a significant ($P < 0.01$) increase in antimycin-A-induced cell death (Fig. 5A). Similarly, Fig. 5B showing changes in cells in pre-G1 indicates the same profile where antimycin A alone caused a significant ($P < 0.05$) increase in apoptosis, whereas IGFBP-3 alone had no effect relative to controls. However, when used together IGFBP-3 caused a significant ($P < 0.05$) increase in antimycin-A-induced apoptosis (Fig. 5B).

IGFBP-5 Has No Effect on an Apoptotic Dose of Antimycin A

We used trypan blue dye exclusion to measure the percentage of dead cells compared to

untreated control cells following treatment with an apoptotic dose of antimycin A alone, IGFBP-5 (100 ng/ml) alone, and the combination of both treatments. Data showed that antimycin A alone caused a significant ($P < 0.001$) increase in dead cells and IGFBP-5 alone had no effect relative to controls. In contrast to IGFBP-3, IGFBP-5 had no effect on antimycin-A-induced cell death (Fig. 6A). Similarly, Figure 6B shows the same profile in pre-G1 peak cells where antimycin A alone caused a significant ($P < 0.05$) increase in apoptosis and IGFBP-5 alone had no effect relative to controls. Similarly, IGFBP-5 had no effect on antimycin-A-induced apoptosis. To show that IGFBP-5 is active in these cell models, we have included data indicating that IGFBP-5 significantly ($P < 0.001$) inhibits C2-induced apoptosis (Fig. 6C).

DISCUSSION

The IGFBPs are a complex family of closely related proteins that act as modulators of IGF availability [Jones and Clemmons, 1995; Oh et al., 1996]. In addition to the ability to both potentiate and inhibit the action of the IGFs [Conover et al., 1990; Conover et al., 1993], it is now clear that a number of IGFBPs can exert IGF-independent effects. We have demonstrated previously that IGFBP-3 has differential effects on physiologic inducers of apoptosis, namely a ceramide analogue (C2) and a synthetic RGD-containing peptide. We found that independent of IGF-I, IGFBP-3 could accentuate C2-induced apoptosis [Gill et al., 1997] but had no effect on that initiated by RGD. However, IGFBP-5 can inhibit both these inducers of apoptosis [Perks et al., 1999a].

The possible mechanisms of these differential IGF-I-independent actions of IGFBP-3 and -5 have been studied. Several groups have ascribed specific binding sites as IGFBP-3 receptors [Oh et al., 1993; Leal et al., 1997] although no linkage between these surface binding sites and intracellular signalling pathways have been demonstrated. It was initially proposed that specific cell surface binding sites for IGFBP-3 existed on Hs578T cells [Oh et al., 1993]. IGFBP-3 binding sites are located on breast cancer cell membranes and it is thought to be the mid-region of the IGFBP-3 molecule that is responsible for such binding [Yamanaka et al., 1999]. In addition, a putative IGFBP-5

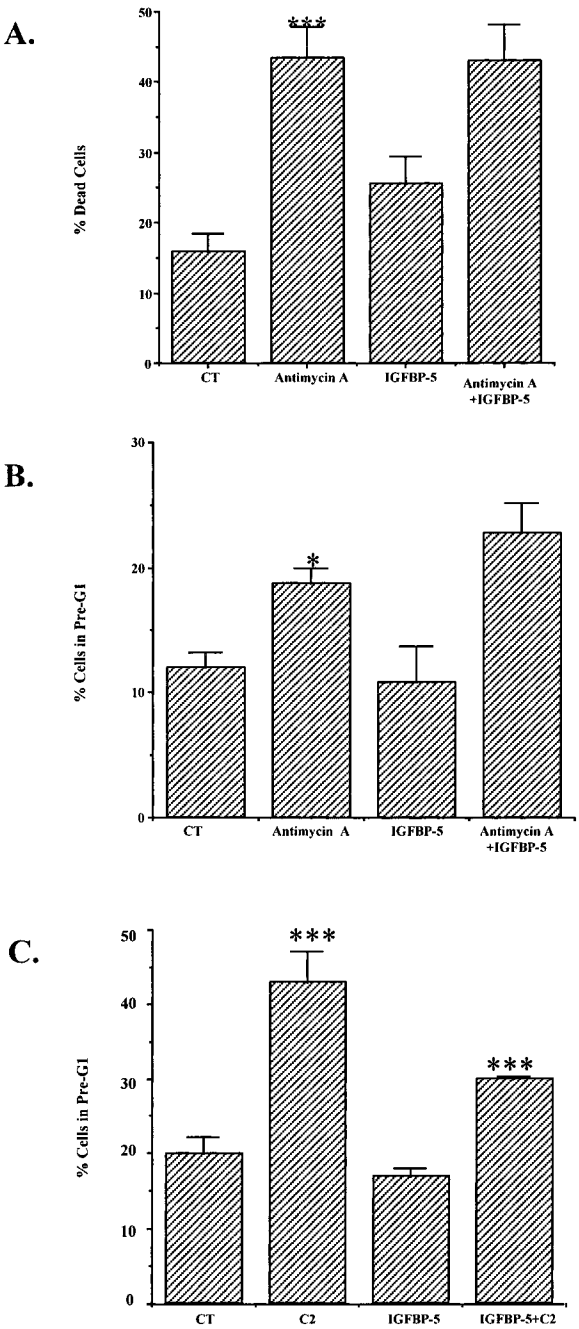

Fig. 6. Insulin-like growth factor binding protein-5 (IGFBP-5) has no effect on an apoptotic dose of antimycin A in the Hs578T human breast cancer cells. Graphs represent the percentage of dead cells (**A**) cells in the pre-G1 peak (**B**) of untreated cells, antimycin A alone (10 μmol/L), IGFBP-5 alone (100 ng/ml), and there is no difference between antimycin A and IGFBP-5 where antimycin A is greater than controls and antimycin A plus IGFBP-5 versus antimycin A alone. **C:** Indicates control cells, an apoptotic dose of ceramide, IGFBP-5 (100 ng/ml), and ceramide plus IGFBP-5 to illustrate that IGFBP-5 is functional. Ceramide is greater than control and ceramide plus IGFBP-5 is less than ceramide. Graphs show the mean of data from at least three experiments that were each performed in triplicate. $^{*}P < 0.05$; and $^{***}P < 0.001$.

receptor has also been described [Andress, 1998].

Another characteristic that is shared by both IGFBP-3 and -5 is that they each contain sequences with the potential for nuclear localisation. Nuclear localisation of IGFBP-3 was originally reported [Jaques et al., 1997]. More recently it was demonstrated that both IGFBP-3 and -5 were taken up into the nucleus of T47D breast cancer cells by a common mechanism [Schedlich et al., 1998]. This suggests that IGFBP-3 or -5 may therefore be able to modulate transcriptional activity, and indeed it has recently been shown that IGFBP-3 can bind with the nuclear retinoid receptor RXR [Liu et al., 1999].

Initially, we characterised the response of the Hs578T cells to antimycin A, establishing both nonapoptotic and apoptotic doses. We then demonstrated that a nonapoptotic dose of antimycin A could dramatically inhibit C2-induced apoptosis. In contrast, it markedly accentuated that caused by RGD. Ceramide-induced cell death has previously been associated with the mitochondria [Esposti and McLennan, 1998]; and in the rat, ceramide-induced hepatocyte cell death was shown to involve disruption of mitochondrial function [Arora et al., 1997]. More recently it has been shown that C2 acts by causing the formation of reactive oxygen intermediates and may affect mitochondrial components directly [Garcia-Ruiz et al., 1997; Gudz et al., 1997; Quillet-Mary et al., 1997].

Our data suggests that the apoptotic effects of C2 appear more dependent on disruption of mitochondrial activity than those initiated by RGD. Our results are in agreement with a recent report that suggests that two main apoptotic pathways exist; either dependent or independent of the mitochondria for its execution [Scaffidi et al., 1999]. These two pathways are not exclusive and can both potentially be activated in the same cells [Nagata, 1999].

We then established an apoptotic dose of antimycin A and demonstrated that IGFBP-3 could accentuate apoptosis initiated at the level of the mitochondria, whereas IGFBP-5 had no effect. We have shown previously that IGFBP-3 can accentuate apoptosis induced by C2 itself [Gill et al., 1997], in addition to accentuating agents such as UV [Hollowood et al., 1999] and paclitaxel [Fowler et al., 1999],

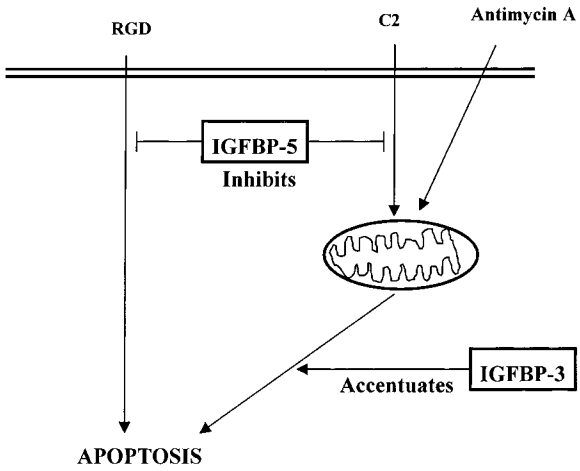

Fig. 7. Interactions of insulin-like growth factor binding protein-3 and -5 with ceramide and arginine-glycine-aspartic acid-induced apoptosis in Hs578T cells.

which also induce apoptosis via generation of endogenous ceramide. However, IGFBP-3 had no effect on apoptosis induced by cell detachment. In direct contrast, IGFBP-5 could rescue cells from both initiators of programmed cell death.

Based on our present findings we further speculate that IGFBP-3 could only accentuate apoptosis induced via pathways incorporating the mitochondria. However, IGFBP-5, which we have shown can inhibit both RGD and C2-induced apoptosis, had no effect on apoptosis initiated by antimycin A. This suggests IGFBP-5 is exerting its effect upstream of, or simply independent of, the mitochondria. These results would fit into a model analogous to the two distinct signalling pathways for apoptosis recently proposed, as summarised in Figure 7 [Nagata et al., 1999].

As outlined above, there is evidence that both IGFBP-3 and IGFBP-5 could interact with specific cell-surface receptors, they are also internalised into the cytoplasm and could be actively transported into the nucleus. There is also evidence supporting many potential interactions with proteases or other ligands on the cell surface. It remains feasible that interactions at any of these sites could be responsible for initiating the described effects on cell survival; with signalling for IGFBP-5 intercepting signalling for apoptosis prior to the mitochondria and signalling for IGFBP-3 acting at or downstream of the mitochondria.

ACKNOWLEDGMENTS

We acknowledge Mr. Paul Newcomb for his technical assistance with the flow cytometry.

REFERENCES

Andress DL. 1998. Insulin-like growth factor binding protein-5 (IGFBP-5) stimulates phosphorylation of the IGFBP-5 receptor. Am J Physiol 274:E744–750.

Arora AS, Jones BJ, Patel TC, Bronk SF, Gores GJ. 1997. Ceramide induces hepatocyte cell death through disruption of mitochondrial function in the rat. Hepatology 25:958–963.

Conover CA, Bale LK, Clarkson JT, Durham SK. 1993. Potentiation of insulin-like growth factor action by insulin-like growth factor binding protein-3: studies of underlying mechanism. Growth Regulation 3:87–88.

Conover CA, Ronk M, Lombana F, Powell DR. 1990. Structural and biological characterisation of bovine insulin-like growth factor binding protein-3. Endocrinology 127: 2795–2803.

Esposti MD, McLennan H. 1998. Mitochondria and cells produce reactive oxygen species in virtual anaerobiosis: relevance to ceramide-induced apoptosis. FEBS Letters 430:338–342.

Fowler CA, Perks CM, Holly JMP, Farndon JR. 1999. IGFBP-3 modulates paclitaxel induced apoptosis in the human breast cancer cells (Hs578T) in an IGF-independent manner. In: Proceedings of the 81st Annual Meeting of the American Endocrine Society. San Diego. p. P2–580.

Freedman VH, Shin S. 1974. Cellular tumorigenicity in nude mice; correlation with cell growth in semisolid medium. Cell 3:353–359.

Frisch SM, Francis H. 1994. Disruption of epithelial cell-matrix interactions induces apoptosis J Cell Biol 124: 619–626.

Garcia-Ruiz C, Colell A, Mari M, Morales A, Fernandez-Checa JC. 1997. Direct effect of ceramide on the mitochondrial electron transport chain leads to generation of reactive oxygen species. Role of mitochondrial glutathione. J Biol Chem 272:11369–11377.

Giancotti FG, Ruoslahti E. 1990. Elevated levels of $\alpha_5\beta_1$, fibronectin receptor suppress the transformed phenotype of CHO cells. Cell 60:849–859.

Gill ZP, Perks CM, Newcomb PV, Holly JMP. 1997. Insulin-like growth factor binding protein (IGFBP-3) predisposes breast cancer cells to programmed cell death in a non-IGF dependent manner. J Biol Chem 272: 25602–25607.

Green DR, Amarante-Mendes GP. 1998. The point of no return: mitochondria, caspases and the committment to cell death. Results Probl Cell Diff 24:45–61.

Gudz TI, Tserng KY, Hoppel CL. 1997. Direct inhibition of mitochondrial respiratory chain complex III by cell-permeable ceramide. J Biol Chem 272:24154–24158.

Hayman EG, Pierschbacher MD, Ruoslahti E. 1985. Detachment of cells from culture substrate by soluble fibronectin peptides. J Cell Biol 100:1948–1954.

Hollowood AD, Lai T, Perks CM, Newcomb PV, Alderson D, Holly JMP. 1999. IGFBP-3 acts in a positive feedback loop to accentuate P53 mediated apoptosis of compromised cells independently of IGF. In: Proceedings of the 81st Annual Meeting of the American Endocrine Society. San Diego p. P2–581.

Ingber DE. 1990. Fibronectin controls capillary endothelial cell growth based on its ability to modulate cell shape. Proc Natl Acad Sci USA 87:3579–3583.

Jaques G, Noll K, Wegmann B, Witten S, Kogan E, Radulescu RT, Havemann K. 1997. Nuclear localization of insulin-like growth factor binding protein 3 in a lung cancer cell line. Endocrinology 138:1767–1770.

Jones JI, Clemmons DR. 1995. Insulin-like growth factors and their binding proteins: biological actions. Endocr Rev 16:3–34.

Knudson KA, Rao PE, Damsky CH, Buck CA. 1981. Membrane glycoproteins involved in cell-substratum interactions. Proc Natl Acad Sci USA 78:6071–6075.

Leal SM, Liu Q, Huang SS, Huang JS. 1997. The type V transforming growth factor beta receptor is the putative insulin-like growth factor-binding protein-3 receptor. J Bio Chem 272:20572–20576.

Lillie RD. 1977. H.J. Conn's biological stains, 9th Edition. Baltimore: Williams and Wilkins Company.

Liu BR, Lee HY, Clifford JL, Kurie JM, Cohen P. 1999. Direct functional interactions between IGFBP-3 and RXR regulate gene expression and cellular apoptosis. In: Proceedings of the 81st Annual Meeting American Endocrine Society. San Diego. p. HT-12.

Nagata S. 1999. Biddable death. Nature Cell Biol 1:E143–E145.

Obeid LM, Linardic CM, Karolak LA, Hannun YA. 1993. Programmed cell death induced by ceramide. Science 259:1769–1771.

Oh Y, Muller HL, Lamson G, Rosenfeld RG. 1993. Insulin-like growth factor (IGF)-independent action of IGF-binding protein-3 in Hs578T human breast cancer cells. Cell surface binding and growth inhibition. J Bio Chem 268:14964–14971.

Oh Y, Nagalla SR, Yamanaka Y, Kim H-S, Wilson E, Rosenfeld RG. 1996. Synthesis and characterisation of insulin-like growth factor-binding protein (IGFBP)-7. J Bio Chem 271:30322–30325.

Perks CM, Bowen S, Gill ZP, Newcomb PV, Holly JMP. 1999a. Differential IGF-independent effects of insulin-like growth factor binding proteins (1-6) on apoptosis of breast epithelial cells. J Cell Biochem 75;652–664.

Perks CM, Gill ZP, Newcomb PV, Holly JMP. 1999b. Effect of insulin-like growth factor binding protein-1 on integrin signalling and the induction of apoptosis in human breast cancer cells. Br J Cancer 79:701–706.

Quillet-Mary A, Jaffrezou JP, Mansat V, Bordier C, Naval J, Laurent G. 1997. Implication of mitochondrial hydrogen peroxide generation in ceramide-induced apoptosis. J Bio Chem 272:21388–21395.

Ruoslahti E, Pierschbacher MD. 1987. New perspectives in cell adhesion. Science 238:491–497.

Scaffidi C, Schmitz I, Zha J, Korsmeyer SJ, Krammer PH, Peter ME. 1999. Differential modulation of apoptosis sensitivity in CD95 type I and type II cells. J Bio Chem 274:22532–22538.

Schedlich LJ, Young TF, Firth SM, Baxter RC. 1998. Insulin-like growth factor-binding protein (IGFBP)-3 and IGFBP-5 share a common nuclear transport pathway in T47D human breast carcinoma cells. J Bio Chem 273:18347–18352.

Tucker RW, Butterfield CE, Folkman J. 1981. Interaction of serum and cell spreading affects growth of neoplastic and nonneoplastic cells. J Supra Struct Cell Biochem 15:29–40.

Wyllie AH. 1980. Cell death: the significance of apoptosis. Int Rev Cytol 60:251–306.

Yamanaka Y, Fowlkes JL, Wilson EM, Rosenfeld RG, Oh Y. 1999. Characterisation of insulin-like growth factor binding protein-3 (IGFBP-3) binding to human breast cancer cells: kinetics of IGFBP-3 binding and identification of receptor binding domain of the IGFBP-3 molecule. Endocrinology 140:1319–1328.

Zhang Z, Huang L, Shulmeister VM, Chi Y-I, Kim KK, Hung L-W, Crofts AR, Berry EA, Kim S-H. 1998. Electron transfer by domain movement in cytochrome bc1. Nature 392:677–684.